Spin pseudogap in $La_{2-x}Sr_xCuO_4$ studied by neutron scattering

C. H. Lee
National Institute of Advanced Industrial Science and Technology, 1-1-1 Umezono, Tsukuba, Ibaraki 305-8568, Japan

K. Yamada
Institute for Chemical Research, Kyoto University, Uji 611-0011, Japan

H. Hiraka, C. R. Venkateswara Rao, and Y. Endoh
Institute for Materials Research, Tohoku University, Sendai 980-8577, Japan

(Received 9 September 2002; revised manuscript received 31 January 2003; published 25 April 2003)

Spin excitations of $La_{2-x}Sr_xCuO_4$ have been studied using inelastic neutron scattering techniques in the energy range of 2 meV$\leqslant\omega\leqslant$12 meV and the temperature range of 8 K$\leqslant T\leqslant$150 K. We observed a signature of a spin pseudogap in the excitation spectrum above T_c for the slightly overdoped sample with $x=0.18$. On heating, the spin pseudogap gradually collapses between $T=80$ and 150 K. For the $x=0.15$ and 0.20, although the visibility of gaplike structure at $T\sim T_c$ is lower compared to the $x=0.18$ sample, the broad bump of $\chi''(\omega)$ appears at $\omega\sim 5$ meV, close to the spin-gap energy at base temperature, suggests the existence of the spin pseudogap in the normal state.

DOI: 10.1103/PhysRevB.67.134521 PACS number(s): 74.72.Dn, 75.40.Gb, 75.50.Ee

I. INTRODUCTION

One of the most remarkable phenomena observed in high-T_c cuprates is the opening of a pseudogap above the superconducting (SC) transition temperature (T_c) in excitations of charge as well as spin. To elucidate the basis of this effect, many experimental studies have been carried out using various techniques including photoemission spectroscopy,[1–5] NMR,[6,7] neutron scattering,[8] and others. Nevertheless, the microscopic origin of the pseudogap remains controversial. Many theoretical models have been proposed based on preformed Cooper pairs or SC pairing fluctuations,[9] the RVB state,[10,11] a precursor to a spin-density-wave state,[12] and the formation of dynamical charge stripes. To reduce the considerable theoretical and experimental confusion regarding the basis of the spin pseudogap, further experimental studies are required.

In principle, pseudogap in magnetic excitations, so-called spin pseudogap, is observable using NMR as well as neutron scattering. Especially, neutron scattering spectroscopy has the unique benefit of being able to detect directly the energy gap as well as the momentum dependence of spin fluctuation. In fact, neutron scattering measurements on the $YBa_2Cu_3O_{6+y}$ (YBCO) system observed a gaplike structure in the energy spectrum of dynamical spin susceptibility $\chi''(\mathbf{q},\omega)$ near the (π,π) position in the normal state.[8] For underdoped $La_{2-x}Sr_xCuO_4$ (LSCO), however, no evidence for the existence of a pseudogap in the normal state nor for a spin gap in the SC state has been obtained.[13,14] In contrast, recent neutron scattering studies of optimally or slightly overdoped LSCO have revealed a well-defined energy gap in the incommensurate spin fluctuations below T_c.[14–17] Although results of our previous neutron scattering study indicated the existence of a spin pseudogap at T_c for slightly overdoped LSCO with $x=0.18$,[14] no systematic examination of this system has been performed.

In the present work, we report a comprehensive study of the magnetic excitations in the normal state of LSCO with $x=0.18$ and 0.20. From a comparison of these results with those arising from the previous measurements on LSCO with $x=0.15$,[14] we conclude that a spin pseudogap does exist in the LSCO system but the visibility or the stability of the gaplike energy spectrum is sensitively affected by the Sr or hole concentration in these samples.

II. EXPERIMENTAL DETAILS

Single crystals of $La_{2-x}Sr_xCuO_4$ ($x=0.15$, 0.18, 0.20) were grown by the traveling solvent floating zone method (TSFZ) using lamp-image furnaces.[18,19] The as-grown single crystals were annealed under oxygen gas-flow at 900 °C for 50 h to remove any oxygen defects. Both $x=0.15$ and $x=0.18$ crystals had been previously used in neutron scattering measurements with some data also being reproduced in the present paper.[14] Onset temperatures of the SC transition measured by SQUID magnetometers under a magnetic field of 10 Oe are 37.5 K for the $x=0.15$ sample, 36.5 K for the $x=0.18$ sample, and 30.0 K for the $x=0.20$ sample (Fig. 1).

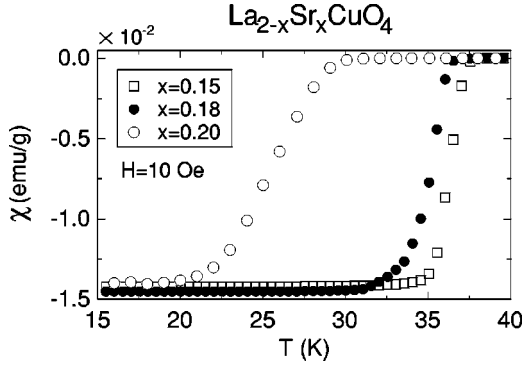

FIG. 1. Shielding signals of $x=0.15$ (open squares), $x=0.18$ (closed circles), and $x=0.20$ (open circles) measured under a magnetic field of $H=10$ Oe.

T_c values for the $x=0.18$ and 0.20 samples are lower than that of the $x=0.15$ sample due to overdoping.

Since T_c is relatively insensitive to Sr concentration near the optimally doped region, we investigated the structural phase transition temperature (T_s) between the high temperature tetragonal (HTT) and low temperature orthorhombic (LTO) phases. The (1,1,0) (in $I4/mmm$ notation) fundamental Bragg peak intensity was monitored as a function of temperature for both $x=0.18$ and 0.20 samples. We note that the intensity changes such as an order parameter upon entering the LTO phase due to the suppression of extinction effects on the neutron beam caused by formation of twinned domain. For the $x=0.15$ sample, intensity of the (0,1,4) (in $Bmab$ notation) superlattice reflection was monitored as a function of temperature. We fitted the observed temperature dependence of the peak intensity using a phenomenological function of $(1-T/T_s)^{2\beta}$, including a Gaussian distribution of T_s (the half width at half maximum of the Gaussian is defined as ΔT_s) to evaluate T_s quantitatively. The index of β was fixed at a value of 0.35. As a result, T_s and ΔT_s were respectively determined to be 191 and 10 K for the $x=0.15$ sample, 111 and 13 K for the $x=0.18$ sample, and 92 and 22 K for the $x=0.20$ sample. Larger ΔT_s for the overdoped sample is due to larger Sr dependence of T_s. Details of sample preparation and characterization have been reported elsewhere.[14,18–20]

Inelastic neutron scattering measurements were performed using the Tohoku University triple-axis spectrometer TOPAN in JRR-3M of JAERI at Tokai. The incident (final) neutron energy was fixed at E_i (E_f)=14.75 or 13.75 meV using the (002) reflection of a pyrolytic graphite monochromator and an analyzer. The typical horizontal collimator sequence was 40′-100′-*S*-60′-80′ or 40′-60′-*S*-60′-80′ where *S* denotes the sample position. A pyrolytic graphite filter and a sapphire crystal were inserted to reduce neutron beam flux from the higher order reflection and high-energy neutrons, respectively. In order to increase the sample volume, two or three single crystalline rods were assembled and mounted in an Al container filled with He thermal exchange gas. A closed cycle ^{4}He refrigerator was used to cool samples down to 8 K with temperatures monitored by a Si diode.

III. ANALYSIS OF NEUTRON SCATTERING EXPERIMENTS

The energy dependence of incommensurate peak intensity is depicted (Fig. 2) after making the following correction on raw data arised from instrument. Background-subtracted inelastic scattering intensities *I*, taken with the E_i-fixed mode are corrected into I' using the following equation:

$$I' = I\frac{\tan\theta_A}{k_f^3}, \tag{1}$$

where k_f and θ_A denote wave number of the scattered neutrons and the analyzer angle, respectively.[21] On the other hand, for experiments with the E_f-fixed mode, the counting time was corrected. This was necessary as the count rate of a fission monitor for the incident beam flux depends on the incident neutron energy due to the energy dependence of intensity of the higher order reflected beam.

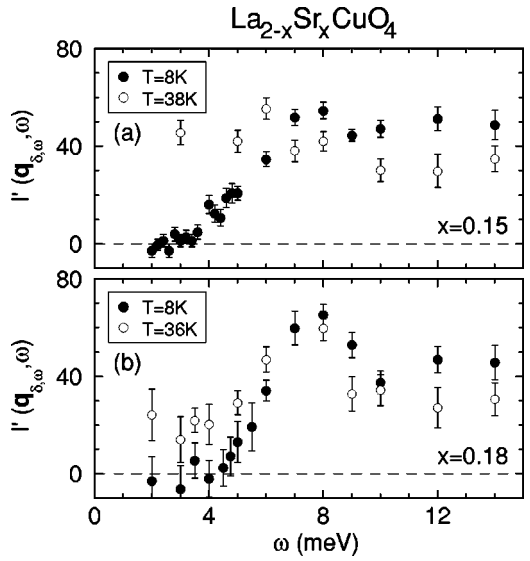

FIG. 2. Energy dependence of the intensity at the incommensurate peak position for (a) $x=0.15$ and (b) $x=0.18$ obtained at $T \ll T_c$ (closed circle) and $T=T_c$ (open circle). Data below $\omega=6$ meV for $x=0.18$ were taken with the E_i fixed mode. Data above $\omega=6$ meV for $x=0.18$ and all data for $x=0.15$ were taken with the E_f fixed mode.

For quantitative analysis, we fitted the observed magnetic intensity, which is proportional to the dynamical structure factor $S(\mathbf{q},\omega)$ and dynamical magnetic susceptibility $\chi''(\mathbf{q},\omega)$ using the following equations convoluted with an instrumental resolution function:

$$S(\mathbf{q},\omega) = \frac{1}{1-\exp\left(-\dfrac{\omega}{k_B T}\right)}\chi''(\mathbf{q},\omega), \tag{2}$$

$$\chi''(\mathbf{q},\omega) = A_\omega \sum_{\delta=1,4}\left\{\frac{\kappa_\omega}{|\mathbf{q}-\mathbf{q}_{\delta,\omega}|^2+\kappa_\omega^2}\right\}, \tag{3}$$

where k_B, $\mathbf{q}_{\delta,\omega}$, κ_ω, and A_ω denote the Boltzman constant, the fourfold positions of incommensurate peaks around (π,π), the q width and a scaling factor, respectively. The absolute values of q-integrated dynamical magnetic susceptibilities $\chi''(\omega)$ are determined using phonon intensities as described previously.[14]

IV. RESULTS

Figure 2 shows energy dependence of incommensurate peak intensity for $x=0.15$ and 0.18. At $T \ll T_c$, both samples have a clear gap spectrum as reported in Refs. 14,15. Upon heating to $T=T_c$, on the other hand, the gap structure is disappeared for $x=0.15$. Whereas, for $x=0.18$, although the intensity does not drop into 0, reduction of peak intensity at low energy region still occurs, which suggests that a spin pseudogap is open. Note that the intensity below $\omega=6$ meV increases with increasing temperature while it de-

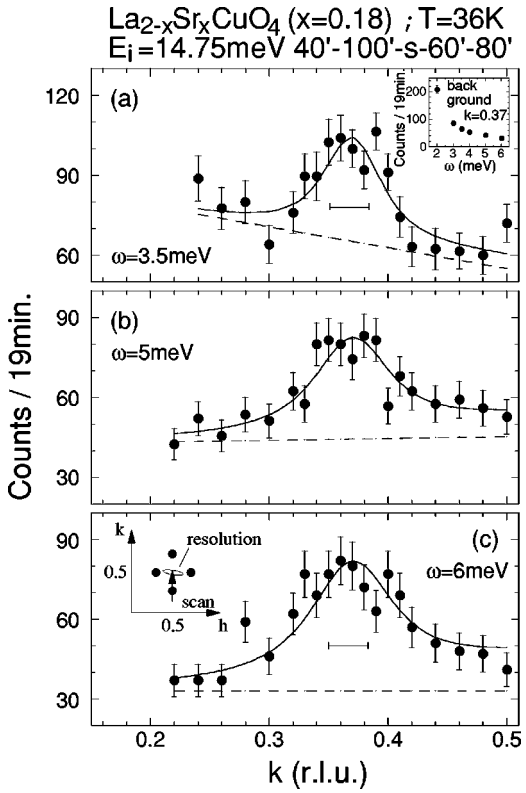

FIG. 3. Energy dependence of the q-spectrum of the incommensurate magnetic signals for $x=0.18$ obtained at $T=T_c$ by a constant energy-scan around (π,π). The scan trajectory and the instrumental resolution ellipsoid are schematically shown in the inset of (c). The incident neutron energy was fixed at $E_i=14.75$ meV. Solid lines are the results of fits convoluted with the instrumental resolution using the background shown by the dashed line (see text for detail). The energy dependence of back ground is depicted in the inset of (a). Horizontal bars depict the instrumental q resolution. The intensity at around (π,π), $k=0.5$ in the figure, reflects the effect of incommensurate peaks located outside of the scan trajectory [see inset of (c)].

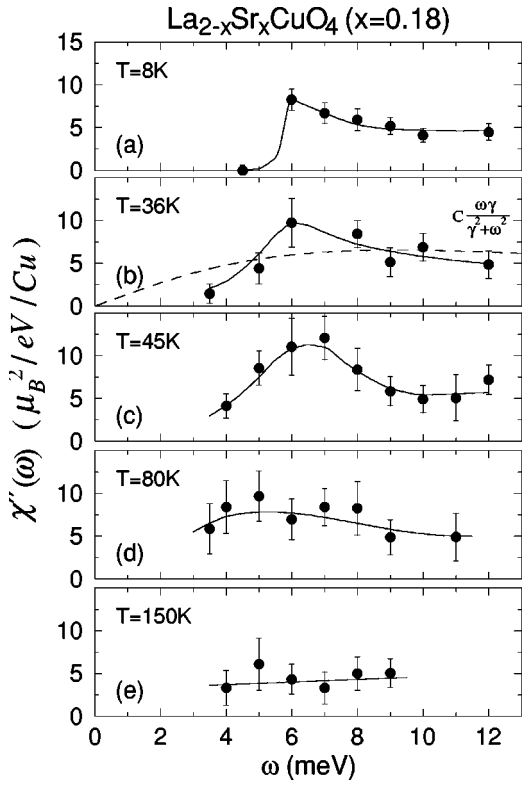

FIG. 4. Energy spectrum of $\chi''(\omega)$ for the $x=0.18$ sample in the temperature range 8 K$\leqslant T\leqslant$150 K. Data below $\omega=6$ meV at $T=8$ and 36 K were taken with the E_i fixed mode and the others with the E_f fixed mode. At $T=36$ and 45 K, a gaplike energy spectrum remains. Solid lines provide guides to the eyes. A dashed line is a fit using Eq. (4).

creases above $\omega=6$ meV, which can be owing to the sum rule.

Typical raw q spectra of magnetic peaks for the $x=0.18$ sample taken by the E_i-fixed mode at $T\sim T_c$ are shown in Fig. 3. Trajectory of the scan is illustrated in the inset of Fig. 3(c). Solid lines depict the results of fits using the scattering function described in Eqs. (2) and (3) convoluted with the resolution function. Long dashed lines depict background. As shown, the solid lines reproduce the observed q spectra quite well. Larger magnetic intensity near the (π,π) position at $\omega=6$ meV than the left side tail dominantly arises from incommensurate peaks outside of the scan trajectory collected by the finite instrumental resolution [see the inset of Fig. 3(c)]. Energy dependence of back ground at incommensurate peak position ($k=0.37$ in Fig. 3) is depicted in the inset of Fig. 3(a). Background at $\omega=3.5$, 5, and 6 meV is estimated from least square fits as shown in Fig. 3. Whereas at $\omega=2$, 3 and 4 meV, it is estimated by taking an average at both sides of the peak tail. The smooth energy dependence suggests that the present background is reasonable. Furthermore we note that if 10 counts larger back ground is used for the data at for example $\omega=6$ meV [Fig. 3(c)], no more reasonable fitting line can be obtained.

Figure 4 shows energy dependence of $\chi''(\omega)$ for the $x=0.18$ sample. As presented in Fig. 4(a) and in our previous paper,[14] the energy spectrum at $T=8$ K exhibits a clear cutoff near $\omega=6$ meV ($E_{\rm gap}$) with a broad bump, while $\chi''(\omega)$ completely vanishes into the background below $\omega\sim4.5$ meV. Upon heating the sample to T_c, magnetic intensities are found to appear below $\omega=4.5$ meV [Figs. 2(b) and 3(a)]. Nevertheless, steep decrease in $\chi''(\omega)$ below $\omega=6$ meV remains, suggesting a presence of a spin pseudogap. The bump around $\omega=6$ meV is also survived. The dashed line in Fig. 4(b) depicts a fit assuming a gapless state using Eq. (4), which details are described in Sec. V. Upon heating the sample to $T=80$ K, the gap-like structure becomes broad, while at $T=150$ K, $\chi''(\omega)$ is nearly independent of temperature, consistent with a collapse of the spin pseudogap.

Figure 5 shows the energy dependence of the linewidth. At $T=8$ K [Fig. 5(a)], the linewidth increases with decreasing the energy down to $\omega=6$ meV. Below the energy gap, the linewidth cannot be defined due to the absence of magnetic intensity. At $T=36$ K, the enhancement around $\omega=6$ meV still remains as a small bump [Fig. 5(b)]. On the other hand, upon heating to $T=80$ K, the width becomes

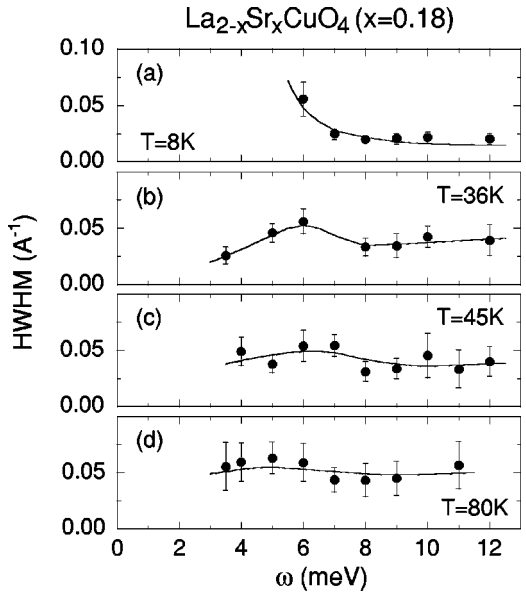

FIG. 5. Energy dependence of the resolution deconvoluted linewidth of an incommensurate peak for the $x=0.18$ sample in the temperature range 8 K$\leqslant T \leqslant$80 K. At $T=8$ K, due to the opening of energy gap, the linewidth is not defined below the gap energy. Solid lines provide guides to the eyes.

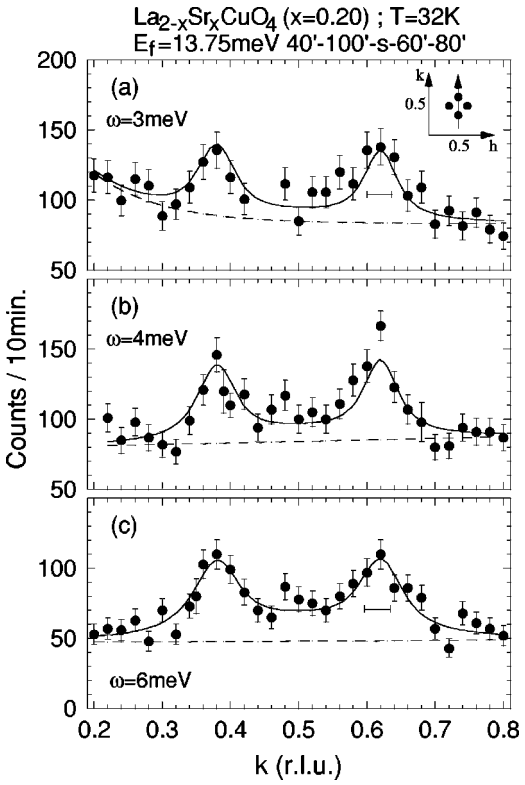

FIG. 6. Energy dependence of the q-spectrum of incommensurate magnetic signals for $x=0.20$ at $T=T_c$. The final neutron energy was fixed at $E_f=13.75$ meV. Solid lines depict the results of fits convoluted with the instrumental resolution using the background shown by the dashed lines.

nearly independent of energy. It seems that the bump near the energy gap disappears with the closing of the spin pseudogap. Possibly, the bump is an effect of the spin pseudogap as discussed in a previous paper.[14]

Figure 6 shows the raw q spectrum of magnetic peaks for the $x=0.20$ sample at $T\sim T_c$ taken at $\omega=3$, 4, and 6 meV under the E_f-fixed mode. Well-defined incommensurate peaks with the peak width similar to that of the $x=0.18$ are observed. We find that the peak intensity has a weaker energy dependence compared to the $x=0.18$ sample. Note that a clear energy gap exists for $T\ll T_c$ [see Fig. 7(a)] with a gap energy of 5–6 meV, which is slightly smaller than that of the $x=0.18$ sample. At $T\sim T_c$, as shown in Fig. 7(d), however, no clear gaplike structure is observed, whereas a weak bump is seen at $\omega\sim E_{\rm gap}$.

Figure 7 summarizes the energy dependences of $\chi''(\omega)$ for the $x=0.15$ (data from Ref. 14), 0.18 and 0.20 samples. At $T=8$ K, all three samples show a well-defined energy gap with a broad maximum near $\omega=6$ meV. Upon heating to $T=T_c$, a gaplike structure of $\chi''(\omega)$ remains only for the $x=0.18$ sample. For the $x=0.15$ and 0.20 samples, $\chi''(\omega)$ decreases linearly with decreasing energy below $\omega\sim 5$ meV, approaching zero only as $\omega\rightarrow 0$. The broad peak in $\chi''(\omega)$, on the other hand, is still observed in all three samples.

V. DISCUSSION

A signature of spin pseudogap in the energy spectrum of incommensurate spin fluctuations was first obtained for the 2-1-4 type hole-doped cuprates. The present neutron scattering experiment shows that a gaplike structure at $T\sim T_c$ is observable only in a narrow Sr concentration range near $x=0.18$. For the $x=0.15$ and 0.20 samples, although a clear gapped spectrum was observed at $T\ll T_c$, the spin pseudogap was poorly defined at $T\sim T_c$.

We first discuss the broad peak in $\chi''(\omega)$ with $\omega\sim 6$ meV in view of the spin pseudogap. In general, for the correlated spin systems without magnetic long range order, $\chi''(\omega)$ exhibits a broad peak even in the normal state. For example, $\chi''(\omega)$ can be described in a Lorentzian form

$$\chi''(\omega)=C\frac{\omega\gamma}{\gamma^2+\omega^2}, \tag{4}$$

where the peak energy nearly corresponds to γ, a characteristic energy scale of spin fluctuations of the system. Thus, the broad peak in $\chi''(\omega)$ does not simply correspond to a spin gap or spin pseudogap. For the optimally doped LSCO, however, $\chi''(\omega)$ has already been studied over a wide energy range by pulse neutron scattering and a broad peak was observed at $\omega=22\sim 40$ meV.[22–24] Then, combining both results from the present low energy experiments and pulse neutron scattering at high energy, there should exist two peaks in $\chi''(\omega)$. A poor fit using Eq. (4) to $\chi''(\omega)$ of $x=0.18$ at $T=36$ K where $\gamma=9$ meV is obtained [Fig. 4(b)] suggests that the $\chi''(\omega)$ at low energy region can not be explained by the simple Lorentizan form. Possibly, the peak at lower energy is the result of forming an energy gap below T_c and even a spin pseudogap at $T\sim T_c$. Figure 8 depicts a concep-

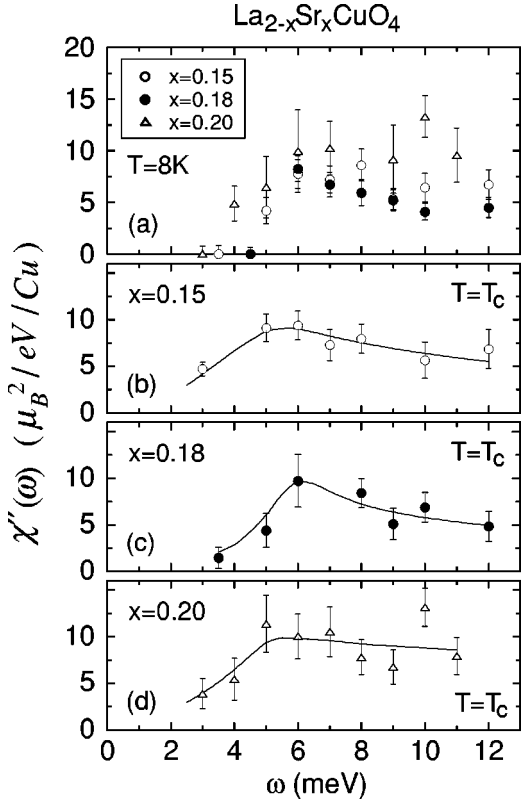

FIG. 7. Energy dependence of $\chi''(\omega)$ for the $x=0.15$, 0.18, and 0.20 samples at (a) $T=8$ K and (b)–(d) $T=T_c$. At $T=8$ K three samples shows clear energy gap with the gap-energy around 6 meV. At $T=T_c$, only the $x=0.18$ sample shows a gaplike energy spectrum. Solid lines provide guides to the eyes.

tual drawing of $\chi''(\omega)$. In normal state, $\chi''(\omega)$ depends linearly on ω at low energies near $\omega=0$. If spin gap or spin pseudogap opens, the $\chi''(\omega)$ near 0 deviates downward from the linear dependence and a bump appears near the gap energy.

According to the fact that the broad peak in $\chi''(\omega)$ with $\omega\sim 6$ meV is also observed in $x=0.15$ and 0.20, we speculate that the spin pseudogap remains at $T\sim T_c$ in these samples although a steep decrease of $\chi''(\omega)$ is less defined. We note that the visibility or the stability of the pseudogap highly depends on the gap-edge structure of the energy spectrum at $T\ll T_c$, which is broader at $x=0.15$ and 0.20 than at $x=0.18$. If gap edge is broader at base temperature, gaplike structure or spin pseudogap is more easily smeared out by heating. Then the spin pseudogap is difficult to detect even if it exists. One possible reason for the gap-edge broadening in the ground state is the spatial distribution of the size of energy gap due to the inhomogeneous carrier distribution and/or chemical potential randomness. The effect of the randomness becomes dominant below $x\sim 0.15$ due to the substantial decrease in the effective carrier concentration.[25] For the $x=0.20$ sample, on the other hand, the spin pseudogap is possibly degradaded by overdoping as reported by many other indirect experiments. At present, however, the direct relation between the stability of spin pseudogap and the gap-edge broadening is not clear.

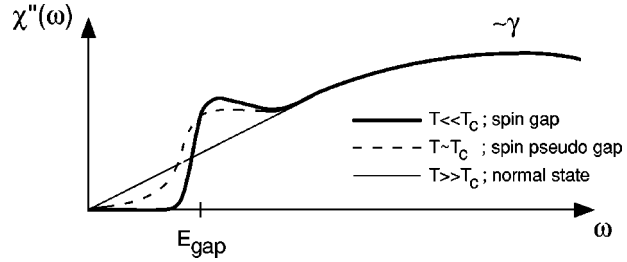

FIG. 8. A conceptual drawing of the q-integrated dynamical magnetic susceptibility $\chi''(\omega)$ in a high-T_c cuprate system with a spin gap, a spin pseudogap, and without a gap. In the normal state well above T_c, $\chi''(\omega)$ exhibits a broad peak near γ, a characteristic energy-scale of spin fluctuations [see text and Eq. (4)], and depends linearly on ω near $\omega=0$. In the superconducting state well below T_c, $\chi''(\omega)$ shows a fully opened gap accompanied by a broad bump near the gap energy (spin-gap shown by the thick solid line). In the intermediate temperature region, we can expect a spin pseudogap state as shown by the broken line in the figure where downward deviation from the linear dependence and the broad bump are observed but the gap is not fully opened.

Many studies on pseudogap have been predicting the existence of two characteristic crossover temperatures T_0 and T^* ($T_0>T^*$). For example, at both temperatures of T_0 and T^*, suppression of magnetic susceptibility and downward deviation of inplane resistivities from linear temperature dependence are observed.[26–28] Furthermore, at T^*, the electronic specific-heat coefficient is slightly suppressed.[29] The origin of such T_0 is interpreted by the onset of antiferromagnetic correlation. Below T^*, on the other hand, the pseudogap is expected to open. According to NMR measurements, the value of T^* for $x=0.20$ is about $T=200$ K.[7] Taking into account the difficulty of determining T^* correctly, the thermal scale of the spin pseudogap observed in the present study appears to be consistent with the results of NMR.

The relation between the pseudogap and superconducting gap is also of great interest. According to angle-resolved photoemission measurements in LSCO, large and small charge pseudogaps exist with magnitudes of about 100 and 30 meV, respectively.[4,5] The present results, however, suggest that a single spin gap structure in the $\chi''(\omega)$ spectrum at base temperatures gradually transforms into the spin pseudogap upon heating.

VI. CONCLUSION

We observed a signature of a spin pseudogap in the energy spectrum of $\chi''(\omega)$ for the slightly overdoped $x=0.18$ samples of LSCO by neutron scattering experiments. Upon heating, the spin pseudogap gradually collapses between $T=80$ and 150 K. For the $x=0.15$ and $x=0.20$ samples, on the other hand, the gaplike structure is poorly defined at $T=T_c$. However, the broad bump in $\chi''(\omega)$ at $T\sim T_c$ suggests the remaining of the spin pseudogap.

ACKNOWLEDGMENTS

The authors would like to thank M. Matsuda , J. M. Tranquada and Y. S. Lee for valuable discussions. The work was

supported by a Grant-In-Aid for Scientific Research on Priority Areas, Novel Quantum Phenomena in Transition Metal Oxides and for Scientific Research (A) from the Ministry of Education, Culture, Sports, Science and Technology of Japan and by a Grant from the Japan Science and Technology Corporation, the Core Research for Evolutional Science and Technology Project and by a Grant from the Ministry of Economy, Trade and Industry of Japan.

[1] H. Ding, T. Yokoya, J. C. Campuzano, T. Takahashi, M. Randeria, M. R. Norman, T. Mochiku, K. Kadowaki, and J. Giapintzakis, Nature (London) **382**, 51 (1996).
[2] A. G. Loeser, Z.-X. Shen, D. S. Dessau, D. S. Marshall, C. H. Park, P. Fournier, and A. Kapitulnik, Science **273**, 3258 (1996).
[3] M. R. Norman, H. Ding, M. Randeria, J. C. Campuzano, T. Yokoya, T. Takeuchi, T. Takahashi, T. Mochiku, K. Kadowaki, P. Guptasarma, and D. G. Hinks, Nature (London) **392**, 157 (1998).
[4] A. Ino, T. Mizokawa, K. Kobayashi, A. Fujimori, T. Sasagawa, T. Kimura, K. Kishio, K. Tamasaku, H. Eisaki, and S. Uchida, Phys. Rev. Lett. **81**, 2124 (1998).
[5] T. Sato, T. Yokoya, Y. Naitoh, T. Takahashi, K. Yamada, and Y. Endoh, Phys. Rev. Lett. **83**, 2254 (1999).
[6] H. Yasuoka, T. Imai and T. Shimizu, *Strong Correlation and Superconductivity*, Springer Series in Solid State Science, Vol. 89, edited by H. Fukuyama, S. Maekawa, and A. P. Malozemoff (Springer-Verlag, New York, 1989).
[7] Y. Itoh, M. Matsumura, and H. Yamagata, J. Phys. Soc. Jpn. **66**, 3383 (1997).
[8] J. Rossat-Mignod, L. P. Regnault, C. Vettier, P. Bourges, P. Burlet, J. Bossy, J. Y. Henry, and G. Lapertot, Physica C **185–189**, 86 (1991).
[9] V. J. Emery and S. A. Kivelson, Nature (London) **374**, 434 (1995).
[10] X. G. Wen and P. A. Lee, Phys. Rev. Lett. **76**, 503 (1996).
[11] Y. Suzumura, Y. Hasegawa, and H. Fukuyama, J. Phys. Soc. Jpn. **57**, 2768 (1988).
[12] D. Pines, Z. Phys. B: Condens. Matter **103**, 129 (1997).
[13] H. Hiraka, Y. Endoh, M. Fujita, Y. S. Lee, J. Kulda, A. Ivanov, and R. J. Birgeneau, J. Phys. Soc. Jpn. **70**, 853 (2001).
[14] C. H. Lee, K. Yamada, Y. Endoh, G. Shirane, R. J. Birgeneau, M. A. Kastner, M. Greven, and Y.-J. Kim, J. Phys. Soc. Jpn. **69**, 1170 (2000).
[15] K. Yamada, S. Wakimoto, G. Shirane, C. H. Lee, M. A. Kastner, S. Hosoya, M. Greven, Y. Endoh, and R. J. Birgeneau, Phys. Rev. Lett. **75**, 1626 (1995).
[16] B. Lake, G. Aeppli, T. E. Mason, A. Schröder, D. F. McMorrow, K. Lefmann, M. Isshiki, M. Nohara, H. Takagi, and S. M. Hayden, Nature (London) **400**, 43 (1999).
[17] S. Petit, A. H. Moudden, B. Hennion, A. Vietkin, and A. Revcolevschi, Physica B **234–236**, 800 (1997).
[18] S. Hosoya, C. H. Lee, S. Wakimoto, K. Yamada, and Y. Endoh, Physica C **235–240**, 547 (1994).
[19] C. H. Lee, N. Kaneko, S. Hosoya, K. Kurahashi, S. Wakimoto, K. Yamada, and Y. Endoh, Semicond. Sci. Technol. **11**, 891 (1998).
[20] C. H. Lee, K. Yamada, M. Arai, S. Wakimoto, S. Hosoya, and Y. Endoh, Physica C **257**, 264 (1996).
[21] N. J. Chesser and J. D. Axe, Acta Crystallogr., Sect. A: Cryst. Phys., Diffr., Theor. Gen. Crystallogr. **29**, 160 (1973).
[22] K. Yamada, Y. Endoh, C. H. Lee, S. Wakimoto, M. Arai, K. Ubukata, M. Fujita, S. Hosoya, and S. M. Bennington, J. Phys. Soc. Jpn. **64**, 2742 (1995).
[23] Y. Endoh, T. Fukuda, S. Wakimoto, M. Arai, K. Yamada, and S. M. Bennington, J. Phys. Soc. Jpn. **69**, 16 (2000).
[24] S. M. Hayden, G. Aeppli, H. A. Mook, T. G. Perring, T. E. Mason, S.-W. Cheong, and Z. Fisk, Phys. Rev. Lett. **76**, 1344 (1996).
[25] Y. Nakamura and S. Uchida, Phys. Rev. B **47**, 8369 (1993).
[26] D. C. Johnston, Phys. Rev. Lett. **62**, 957 (1989).
[27] T. Nakano, M. Oda, C. Manabe, N. Momono, Y. Miura, and M. Ido, Phys. Rev. B **49**, 16 000 (1994).
[28] T. Nakano, N. Momono, M. Oda, and M. Ido, J. Phys. Soc. Jpn. **67**, 2622 (1998).
[29] T. Matsuzaki, M. Ido, N. Momono, R. M. Dipasupil, T. Nagata, A. Sakai, and M. Oda, J. Phys. Chem. Solids **62**, 29 (2001).